J Neurol (2007)
DOI 10.1007/s00415-006-0468-5

ORIGINAL PAPER

Yukihisa Suzuki
Shoichi Mizoguchi
Motohiro Kiyosawa
Manabu Mochizuki
Kiichi Ishiwata
Masato Wakakura
Kenji Ishii

Glucose hypermetabolism in the thalamus of patients with essential blepharospasm

Received: 1 January 2006
Received in revised form: 6 September 2006
Accepted: 11 September 2006
Published online: 26 February 2007

Supported by a generous grant from the Benign Essential Blepharospasm Foundation and Grant-in-Aid for Scientific Research (18991310).

Y. Suzuki, MD, PhD
S. Mizoguchi, MD, PhD
M. Kiyosawa, MD, PhD
M. Mochizuki, MD, PhD
Dept. of Ophthalmology and Visual Science
Tokyo Medical and Dental University
Tokyo, Japan

K. Ishiwata, PhD · K. Ishii, MD (✉)
Y. Suzuki, MD, PhD
S. Mizoguchi, MD, PhD
Positron Medical Center
Tokyo Metropolitan Institute
of Gerontology
35-2 Sakaecho
Itabashi, Tokyo, Japan
Tel.: +81-3/3964-3241, ext. 3503
Fax: +81-3/3964-2188
E-Mail: ishii@pet.tmig.or.jp

M. Wakakura, MD, PhD
Inouye Eye Hospital
Tokyo, Japan

Abstract Essential blepharospasm (EB) is classified as a form of focal dystonia characterized by involuntary spasms of the musculature of the upper face. The basic neurological process causing EB is not known. The purpose of this study was to investigate cerebral glucose metabolism in patients with EB whose symptoms were suppressed by an injection of botulinum-A toxin. Earlier studies were confounded by sensory feedback activities derived from dystonic symptom itself. Cerebral glucose metabolism was examined by positron emission tomography (PET) with ^{18}F-fluorodeoxyglucose (FDG) in 25 patients (8 men and 17 women; age 52.6 ± 10.1 years) with EB. The patients were awake but with the spasms suppressed by an injection of botulinum-A toxin. Thirty-eight normal volunteers (14 men and 24 women; age 58.2 ± 7.3 years) were examined as controls. The difference between the two groups was examined by statistical parametric mapping (SPM99). A significant increase in the glucose metabolism was detected in the thalamus and pons in the EB patients. Hyperactivity in the thalamus may be a key pathophysiological change common to EB and other types of focal dystonia. The activity of the striatum and cerebellum are likely to be sensory dependent.

Key words essential blepharospasm · focal dystonia · glucose metabolism · positron emission tomography · thalamus

Introduction

Essential blepharospasm (EB) is a form of focal dystonia characterized by involuntary spasms of the musculature of the upper face. Earlier studies have reported a glucose hypermetabolism in the thalamus and basal ganglia in patients with dystonia, and it has been widely held that dysfunction of cortical-striato-thalamo-cortical motor circuits may have a major role in the pathophysiology of dystonia [1]. It has also been reported that dystonia is caused by thalamic infarctions [2], and patients with EB have been reported to be associated with increased glucose metabolism in the thalamus [3] and cerebellum [4] by positron emission tomography (PET) studies using ^{18}F-fluorodeoxyglucose (FDG).

There have been several studies on other forms of focal dystonia using PET. In patients with spasmodic torticollis, Galardi et al. reported hypermetabolism in the thalamus, basal ganglia, anterior cingulate gyrus,

JON 2468

and cerebellum [5], and Eidelberg et al. found a relative increase of metabolic activity in the lentiform nucleus and premotor cortices of patients with idiopathic torsion dystonia [6]. In EB and other dystonias, the majority of the studies have demonstrated a hypermetabolism of the thalamus and basal ganglia. A common limitation of earlier neuroimaging studies of dystonia lies in that they observed integral brain activities reflecting both the cause and the consequence of abnormal involuntary movements.

In order to separate the effects of cause and consequence on EB, Hutchinson et al. measured the glucose metabolism of EB patients during wakefulness and during induced sleep because the involuntary movements disappear during sleep. They found a hypermetabolism in the cerebellum and pons only during wakefulness [4]. However they could not find the primary cause of EB during sleep.

We hypothesized that the hyperactivity in the thalamus and basal ganglia is not a secondary phenomenon accompanies the abnormal movement, but is a primary pathophysiological condition that cause the symptoms. To test this hypothesis and to determine the responsible cerebral regions, PET measurements were made to evaluate regional cerebral glucose metabolism while the patients were awake, but the involuntary eyelid movements were suppressed by a botulinum toxin-A injection.

Materials and methods

Twenty-five patients (8 men and 17 women; age 52.6 ± 10.1 years), who visited the Ophthalmology Outpatient Clinic of Tokyo Medical and Dental University Hospital and were diagnosed with bilateral EB, were studied. The mean duration of their illness was 2.9 ± 3.3 years. None had an organic brain disorder or other neuro-psychiatric disease as evaluated by neurologists from conventional diagnostic magnetic resonance images (MRIs). No one had a family history of dystonic disorders. Patients who had not taken any neuro-psychiatric drugs such as neuroleptic drugs, antidepressant drugs, anti-Parkisonian drugs, and anti-epileptic drugs were selected by careful history taking to exclude drug-related cases because drug related cases might confound [7]. Thirty-eight normal volunteers (14 men and 24 women; age 58.2 ± 7.3 years) were recruited as the normal control group. Normal subjects had no organic brain disorders or neuro-psychiatric disease, and had not taken any neuro-psychiatric drugs.

Informed consents were obtained from all the subjects before participation in the PET study. This study protocol was approved by the Institutional Ethics Committee. All of the procedures conformed to the tenets of the Declaration of Helsinki.

All of the patients received an injection of botulinum-A toxin (18 to 36 units bilaterally) into the orbicularis oculi (OO) muscle, and the PET scans were obtained when the spasms of the OO were effectively restrained. PET scanning was done in the time when the spasm of eyelids was depressed after the botulinum toxin treatments within three months. The severity of blepharospasm was assessed with the 0 to 4 (0 = absent, 4 = most severe), and the frequency of blepharospasm was assessed with the 0 to 4 (0 = none, 4 = persistent eye closure), too in accordance with the classification of Jankovic [8]. We evaluated the severity and frequency of the spasm in all the patients before the latest treatment of botulinum toxin and at the time of the PET study, actually between the injection of FDG and the scanning (Table 1). As not all the patients have reached complete suppression of blepharospasm at the moment of PET scan by botulinum-A toxin treatment, we divided the patients into two subgroups for further analysis, based on the on-site evaluation of the blepharospasm symptom: complete suppression group (n = 12; 5 men and 7 women; age 56.2 ± 9.5 years, severity 0, frequency 0) and incomplete suppression group (n = 13, 3 men and 10 women; age 48.8 ± 8.4 years, severity 1 ± 1, frequency 1 ± 1). There was no significant difference in symptomatic scores before treatment between incomplete suppression group (3.00, 3.00), and complete suppression group (3.08, 2.83). The only significant difference ($p < 0.05$) was the duration of illness: 1.50 ± 1.2 years in complete suppression group and 4.15 ± 4.1 years in incomplete suppression group.

MRI scans were obtained from all of the subjects to screen for organic brain disorders with a 1.5 Tesla scanner Signa Horizon (General Electric, Milwaukee). Transaxial images with T1-weighted contrast (3DSPGR, TR = 9.2 ms, TE = 2.0 ms, matrix size = 256 × 256 × 124, voxel size = 0.94 × 0.94 × 1.3 mm), and T2-weighted contrast (First Spin Echo, TR = 3,000 ms, TE = 100 ms, matrix size = 256 × 256 × 20, voxel size = 0.7 × 0.7 × 6.5 mm) were obtained. None of the subjects showed any abnormalities in brain morphology and intensities.

PET data acquisition

PET scans were obtained with the Headtome-V scanner SET 2400W (Shimadzu, Kyoto, Japan) at the Positron Medical Center, Tokyo Metropolitan Institute of Gerontology. Attenuation was corrected by a transmission scan with a $^{68}Ga/^{68}Ge$ rotating source. For the PET scan, a bolus of 120 MBq FDG was injected intravenously. Each patient was then requested to lie down comfortably with their eyes closed. A 6-minute emission scan in 3D acquisition mode was started 45 minutes after the injection, and 50 transaxial images with an interslice interval of 3.125 mm were obtained. The tomographic images were reconstructed using a filtered backprojection method, and Butterworth filter (cutoff frequency 1.25 cycle/cm and order of 2).

Data processing and statistical analysis

PET images were processed and analyzed with the statistical parametric mapping (SPM99) software [9] implemented in Matlab (Mathworks., Sherborn, MA, USA). Statistical parametric maps combine the general linear model and the theoretical Gaussian fields to make statistical inferences about regional effects. All PET images were spatially normalized to a standard template produced by Montreal Neurological Institute using the housemade template of FDG-PET images and smoothed with Gaussian filter for 16 mm FWHM to increase the signal to noise ratio before statistical processing.

After the appropriate design matrix was specified, the subject and group effects were estimated according to the general linear model at each voxel. We selected (compare-populations: 1 scan/subjects (two sample t-test)) in design type, and selected (global normalsation proportional scaling) in global normalization [10]. Statistical inference on the SPM (Z) was corrected using the theory of Gaussian Fields. To test hypotheses about regionally specific group effects, the estimates were compared using linear contrast. The threshold for SPM (Z) was set at $p < 0.05$ with a correction ($p < 0.05$, corrected) for the comparison between whole patient group and normal control group. We compared each of incomplete suppression group and complete suppression group to the normal control group in order to examine the effect of residual spasm. We also directly compared two subgroups each other. The threshold for SPM (Z) for the subgroup comparison was set at ($p < 0.0001$, uncorrected).

Table 1 Strength of the spasm of eyelids in EB patients

Age	Sex	Duration	Term from treatment to PET scanning	Strength of the spasm of eyelids (severity, frequency)			
				Before botulinum toxin treatment		At the time of PET scanning	
62	F	4 years	3 months	R (3, 3)	L (3, 3)	R (1, 1)	L (1, 1)
72	F	1 year	3 months	R (3, 3)	L (3, 3)	R (1, 1)	L (1, 1)
69	M	2 years	3 months	R (3, 3)	L (3, 3)	R (1, 1)	L (1, 1)
45	M	1 year	3 months	R (3, 3)	L (3, 3)	R (1, 1)	L (1, 1)
36	F	1 year	3 months	R (3, 3)	L (3, 3)	R (1, 1)	L (1, 1)
50	F	1 year	3 months	R (3, 3)	L (3, 3)	R (1, 1)	L (1, 1)
60	F	10 years	1 month	R (3, 3)	L (3, 3)	R (1, 1)	L (1, 1)
58	F	10 years	1 month	R (3, 3)	L (3, 3)	R (1, 1)	L (1, 1)
58	F	5 years	2 months	R (3, 3)	L (3, 3)	R (0, 0)	L (0, 0)
57	F	1 year	3 months	R (3, 3)	L (3, 3)	R (1, 1)	L (1, 1)
50	F	2 years	3 months	R (4, 3)	L (4, 3)	R (0, 0)	L (0, 0)
46	M	1 year	3 months	R (4, 3)	L (4, 3)	R (0, 0)	L (0, 0)
40	M	1 year	3 months	R (3, 3)	L (3, 3)	R (0, 0)	L (0, 0)
58	F	2 years	3 months	R (3, 3)	L (3, 3)	R (1, 1)	L (1, 1)
59	F	10 years	3 months	R (3, 3)	L (3, 3)	R (1, 1)	L (1, 1)
54	F	1 year	3 months	R (4, 3)	L (4, 3)	R (0, 0)	L (0, 0)
53	M	1 year	1 month	R (3, 3)	L (3, 3)	R (0, 0)	L (0, 0)
45	F	1 year	1 month	R (3, 3)	L (3, 3)	R (0, 0)	L (0, 0)
56	F	1 year	3 months	R (2, 2)	L (2, 2)	R (0, 0)	L (0, 0)
57	F	1 year	3 months	R (3, 3)	L (3, 3)	R (0, 0)	L (0, 0)
50	F	10 years	3 months	R (3, 3)	L (3, 3)	R (1, 1)	L (1, 1)
38	M	2 years	3 months	R (3, 3)	L (3, 3)	R (0, 0)	L (0, 0)
33	F	10 months	3 months	R (2, 2)	L (2, 2)	R (0, 0)	L (0, 0)
55	M	1 year	3 months	R (3, 3)	L (3, 3)	R (1, 1)	L (1, 1)
56	M	1 year	3 months	R (3, 3)	L (3, 3)	R (0, 0)	L (0, 0)
Average							
Incomp group	4.2 ± 4.1 years			R (3.00, 3.00)	L (3.00, 3.00)		
Comp group	1.5 ± 1.2 years			R (3.08, 2.83)	L (3.08, 2.83)		
Total	2.9 ± 3.3 years			R (3.04, 2.92) L (3.04, 2.92)	R (0.52, 0.52) L (0.52, 0.52)		

Severity of spasm was rated on 0 (=none) to 4 (=severe) scale[8]
Frequency of spasm was rated on 0 (=none) to 4 (=functionally blind) scale[8]
Incomp Group: incomplete suppression group
Comp Group: complete suppression group

Results

A regional glucose hypermetabolism was found in the thalamus and pons bilaterally in patients with EB ($p < 0.05$, corrected), whose eyelid spasms were decreased by botulinum-A toxin (Table 2, Fig. 1). We made mean PET images of all patients and all normal subjects. Regions of interest (ROIs), 1 cm diameter circles, were placed the thalamus and pons, respectively, due to measure the glucose metabolism levels of these regions. The mean increases were 6.5% in the thalamus and 5.3% in the pons. A trend of glucose hypermetabolism was also found in the putamen bilaterally in EB patients, but the increase was not significant ($p < 0.01$, uncorrected). There was no regional glucose hypometabolism above the statistical significant level. We found that significant hypermetabolism in the thalamus, pons and cerebellum bilaterally in incomplete suppression group

Table 2 Areas and coordinates for the maxima of regional glucose hypermetabolism in essential blepharospasm patients

Area	X	Y	Z	Z score
Thalamus (R)	12	−20	−2	5.00
Thalamus (L)	−8	−22	−2	5.54
Pons (R)	6	−40	−34	4.47
Pons (L)	−12	−40	−34	4.83

Areas with $Z \geq 4.17$ ($p < 0.05$, corrected) were listed

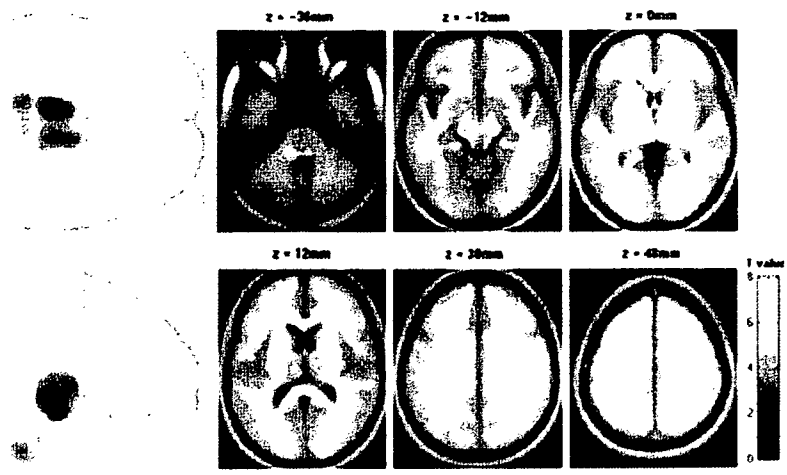

Fig. 1 Areas of glucose hypermetabolism in patients with essential blepharospasm are showed ($p < 0.05$, corrected). Left; Sagittal and transverse views of a statistical parametric map (SPM) rendered into standard stereotactic space and projected onto a glass brain. Right; Six axial slices of brain are shown. The left side of the figure corresponds to the left hemisphere

($p < 0.0001$, uncorrected) (Table 3A, Fig. 2). On the other hand, hypermetabolism was observed only in the bilateral thalamus in complete suppression group ($p < 0.0001$, uncorrected) (Table 3B, Fig. 2). However, we could not find any significant difference between incomplete suppression group and complete suppression group by direct comparison ($p < 0.001$, uncorrected).

Discussion

Effect of involuntary movements

A majority of the studies on EB and other dystonias have demonstrated hypermetabolism of the thalamus and basal ganglia, however, there is a problem in interpreting these results because these studies were performed while the patients had active symptoms of dystonia, e.g., involuntary eyelid movements in EB patients. Thus, the observed abnormal cerebral activities could be due not only to the primary cause of the dystonia, but also to the sensory input secondary from the involuntary movements. To overcome this criticism in EB patients, it is necessary to suppress the spasms of the eyelids. Hutchinson et al. hypothesized that there is metabolic increase in the thalamus and basal ganglia in EB patients because of an overactivity of a cortico-striato-thalamo-cortical motor circuit, and measured the glucose metabolism of 6 EB patients by PET while they were awake with active symptoms and while they were asleep without symptoms [4]. They found hypermetabolism in the cerebellum and pons during wakefulness, but not in the thalamus and basal ganglia during either condition. We suggest two possible reasons why they miss the hyperactivity in the thalamus and basal ganglia. First, the number of the patients and normal subjects in their study might not be enough. The difference of mean between two groups was relatively small compared to the standard deviation (difference of mean = 3.5, SD = 4.8 in the thalamus, for example), we have to increase the number of subject more than 20 to get a consistent statistical significance. Second,

Table 3 Areas and coordinates for the maxima of regional glucose hypermetabolism in incomplete suppression EB patients

Area	x	y	z	Z score
A				
Thalamus (R)	12	−10	2	3.52
Thalamus (L)	−6	−22	2	3.70
Pons (R)	2	−40	−32	5.06
Pons (L)	−6	−44	−32	5.16
Cerebellum (R)	40	−38	−38	3.58
Cerebellum (L)	−50	−48	−46	3.84
B				
Thalamus (R)	14	−20	−2	3.93
Thalamus (L)	−10	−20	−2	4.20

Areas with $Z \geq 3.45$ ($p < 0.0001$, uncorrected) were listed

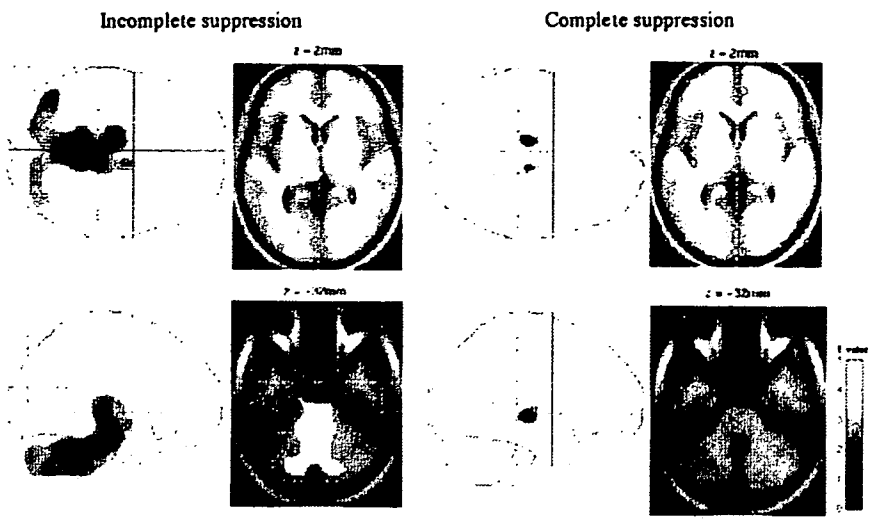

Fig. 2 Areas of glucose hypermetabolism in EB patients with incomplete suppression (left) and complete suppression (right) by botulinum toxin treatment are showed ($p < 0.0001$, uncorrected)

sleep might have depressed not only the involuntary movements but also the primary functional alteration in the brain of EB.

Ceballos-Baumann et al. examined patients with writer's cramp by PET during writing words before and after botulinum toxin treatment [11]. They found higher cerebral blood flow of patients before and after botulinum-toxin in the thalamus, left insula, bilateral premotor cortex, and bilateral primary sensory cortex than in normal subjects. In patients, activation in the cerebeller vermis was found before botulinum-toxin, but the activation disappeared after the treatment. We suggest that they succeeded in reducing the effect of involuntary movement, although the voluntary movements may still be a confounding factor.

Because the botulinum-toxin inhibits neuro-muscular conduction by a presynaptic blockade, we expected that the botulinum-toxin has minimum influence on the central causative mechanism of EB. Several previous studies have reported no significant alterations in the level of cerebral blood flow after botulinum toxin treatment [11, 12]. Therefore, in the present study, we performed a PET study in a larger size of the patients while awake and their spasms were effectively suppressed by the injection of botulinum toxin into the OO muscle bilaterally: 25 EB subjects and 38 normal controls. Under these conditions, we found a significant glucose hypermetabolism in the thalamus bilaterally in EB patients ($P < 0.05$, corrected).

Incomplete suppression group and complete suppression group

We divided EB patients to incomplete suppression group (13 patients) and complete suppression group (12 patients) based on the scores of blepharospasm at the PET scanning. There was no significant difference in severity and frequency of spasm before treatment between these 2 groups. However, the mean duration of illness of incomplete suppression group was significantly longer than that of complete suppression group. Incomplete suppression group contained 4 patients whose duration of illness was over 10 years. These patients have repeatedly been treated by botulinum toxin for a long periods. The efficacy of the treatment might have been weakened due to tolerance [13].

Regional glucose metabolism in patients with EB

Hypermetabolism in the thalamus, basal ganglia, anterior cingulate gyrus and cerebellum of patients with spasmodic torticollis using PET were reported [5]. The results of functional imaging studies are often interpreted using the present anatomical model of information flow in cortico-striato-thalamo-cortical motor circuit (Fig. 3) [14]. Based on this model, there are three possible points which might alter thalamic activity. All of them are the alterations in inhibitory synaptic functions mediated by GABAergic system. Recent reports suggest that altered GABAergic inhibition may play a role in the symptomatology of dystonia. Previous studies found a reduction of GABA levels in the sensorimotor cortex and striatum of patients with focal dystonia [16]. We suspect that a reduction of GABA levels in the striatum or thalamus might cause the hyperactivity in these areas.

Macia et al. reported that injection of bicuculline, an antagonist to $GABA_A$, into the monkey thalamus induced dystonic symptoms contralaterally and found an overactivity of thalamic neurons ipsilateral to the treatment [17]. On the other hand, Kaji reported that one of the important functions of basal ganglia is the

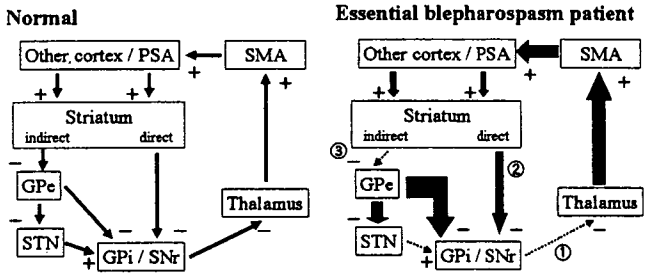

Fig. 3 Principal pathways of the normal corticobasal ganglia-cortical loops and hypothetical alterations. In the normal loops (left), the striatum receives input from the primary somatosensory area (PSA) and from other areas of the motor and sensory cortex. The striatum projects by direct and indirect pathways to the major output structures of the basal ganglia, the globus pallidus interna (GPi) and substantia nigra reticulate (SNr). An indirect pathway includes a striatal-globus pallidus externa (GPe) projection. Some GPe fibers project to the subthalamic nucleus (STN) and GPi/SNr, and other fibers project directly to the GPi/SNr. GPi/SNr, which in turn, projects to the thalamus with a subsequent feedback to motor cortex, primarily the SMA. The effect of each structure on subsequent structures is to increase (+) or decrease (−) neuronal activity as indicated, adapted from Tempel et al. [14] and Garfen [15]. For glucose hypermetabolism in the thalamus and striatum of EB patients (right), the possible points of impairments with the circuit are; 1) to impaired inhibition from GPi/SNr, 2) decreased GPi/SNr activity may result in increased activity of the direct pathway from Striatum to GPi/SNr, and 3) impaired the indirect pathway at the level of Striatum-GPe connection

gating of sensory input for motor control [18], and its alteration might cause dystonia. Previous reports found glucose hypermetabolism in EB and other focal dystonias in the striatum as well as in the thalamus [3, 5]. Recently, Schmidt et al. reported that a subregion of the putamen was active during EB spasms in patients but not during voluntary blinks in normal subjects using fMRI [19]. Perlmutter et al. have demonstrated that individuals with EB and hand dystonia have a reduced level of dopamine D_2-like receptors in the putamen relative to control subjects [20], suggesting that dopamine D_2-receptor loss disrupts lateral inhibition created by the indirect pathway of the basal ganglia. These evidences have suggested that the altered function of the putamen may be a critical component of EB. We found a trend of glucose hypermetabolism in the putamen bilaterally in EB patients, but the increase was not significant ($p < 0.01$, uncorrected). It is plausible that the hyperactivity of the striatum is sensory-input dependent. On the other hand, the hyperactivity in the thalamus was more consistent even with the depletion of sensory feedback. From these observations, hyperactivation of the thalamus may be one of the primary causes of EB, however, it might reflect a compensatory mechanism. Further investigation is required to clarify the different role of the thalamus and the striatum in the pathophysiological mechanism of EB.

We found significant hypermetabolism in the cerebellum and pons in incomplete suppression group ($p < 0.0001$, uncorrected), and not in complete suppression group ($p < 0.0001$, uncorrected) when the images of these groups were contrasted to the control group. We did not find significant difference by direct comparison of subgroups, presumably because the number of the patients in these subgroups might not be enough to reach statistical significance. The cerebellum receives extensive somatosensory input via spinocerebellar pathways, and the cerebellum would be a sensory organ [21]. Hutchinson et al. reported that EB patients exhibit hypermetabolism of the cerebellum and pons during wakefulness, but not during sleeping using PET [4]. And, Ceballos-Baumann et al. reported that patients with writer's cramp activation in the cerebeller vermis was found before botulinum-toxin, but the activation disappeared after the treatment [11]. Our results indicate that activation of the cerebellum in EB patients could be due to increased sensory input derived from involuntary muscle contraction of eyelids. Aramideh et al. reported a secondary blepharospasm patient with a small dorsomedial pontine lesion [22], and LeDoux et al. reported a secondary cervical dystonia patients due to infarctions or hemorrhage in the pons [23]. They hypothesized that abnormalities of olivocerebellar circuit and cortico-striato-thalamo-cortical motor circuit might produce similar movement disorders, and they suggested that lesions in the pons obstructed the cerebellar afferent pathways, and produced cervical dystonia.

We found significant hypermetabolism of the tegmentum in the inferior pons, and this area corresponds to the facial nucleus and facial nerve. The facial nerve is the final output pathway of focal facial dystonia from the nervous system. As the effect of botulinum-A toxin is peripheral, the facial nuclei and related structure in pons may remain hyperactive even after the treatment as we observe in our results. From these things, we suspected that hypermetabolism in the cerebellum and pons was the secondary phenomenon related to muscular activity of eyelids.

Conclusions

A glucose hypermetabolism was detected in the thalamus and pons bilaterally in EB patients. Hyperactivity in the thalamus may be related to the primary cause of compensatory mechanism of EB sharing the common pathophysiological mechanism to other types of focal dystonia.

Acknowledgements This work was supported by a generous grant from the Benign Essential Blepharospasm Ressearch Foundation. The authors thank Dr. K. Kawamura, Dr. K. Oda, and Ms. M. Ando for technical support.

References

1. Berardelli A, Rothwell JC, Hallett M, Thompson PD, Manfredi M, Marsden CD (1998) The pathophysiology of primary dystonia. Brain 121:1195–1212
2. Kostic VS, Stojanovic-Svetel M, Kacar A (1996) Symptomatic dystonias associated with structural brain lesions: report of 16 cases. Can J Neurol Sci 23:53–56
3. Esmaeli GB, Nahmias C, Thompson M, et al. (1999) Positron emission tomography in patients with benign essential blepharospasm. Ophthal Plast and Reconstr Surg 15:23–27
4. Hutchinson M, Nakamura T, Moeller JR, et al. (2000) The metabolic topography of essential blepharospasm. A focal dystonia with general implications. Neurology 55:673–677
5. Galardi G, Perani D, Grassi F, et al. (1996) Basal ganglia and thalamo-cortical hypermetabolism in patients with spasmodic torticollis. Acta Neurol Scand 94:172–176
6. Eidelberg D, Moeller JR, Ishikawa T, et al. (1995) The metabolic topography of idiopathic torsion dystonia. Brain 118:1473–1484
7. Wakakura M, Tsubouchi T, Inouye J (2004) Etizolam and benzodiazepine induced blepharospasm. J Neurol Neurosurg Psychiatry 75:506–509
8. Jankovic J, Orman J (1987) Botulinum A toxin for cranial-cervical dystonia: A double-blind, placebo-controlled study. Neurology 37:616–623
9. Friston KJ, Frith CD, Liddle PF, Frackowiak RS (1991) Comparing functional (PET) images: the assessment of significant change. J Cereb Blood Flow Metab 11:690–699
10. Friston KJ, Frith CD, Liddle PF, Dolan RJ, Lammertsma AA, Frackowiak RSJ (1990) The relationship between global and local changes in PET scans. J Cereb Blood Flow Metab 10:458–466
11. Ceballos-Baumann AO, Sheean G, Passingham RE, et al. (1997) Botulinum toxin does not reverse the cortical dysfunction associated with writer's cramp. A PET study. Brain 120:571–580
12. Ridding MC, Sheean G, Rothwell JC (1995) Changes in the balance between motor cortical excitation and inhibition in focal, task specific dystonia. J Neurol Neurosurg Psychiatry 59:493–498
13. Hsiung GY, Das SK, Ranawaya R, Lafontaine AL, Suchowersky O (2002) Long-term efficacy of botulinum toxin A in treatment of various movement disorders over a 10-year period. Mov Disord 17:1288–1293
14. Tempel LW, Perlmutter JS (1993) Abnormal cortical responses in patients with writer's cramp. Neurology 43:2252–2257
15. Garfen CR (1992) The neostriatal mosaic: multiple levels of compartmental organization. Trends Neurosci 15:133–139
16. Levy LM, Hallett M (2002) Impaired brain GABA in focal dystonia. Ann Neurol 51:93–101
17. Macia F, Escola L, Guehl D, Michelet T, Bioulac B, Burbaud P (2002) Neuronal activity in the monkey motor thalamus during bicuculline-induced dystonia. Eur J Neurosci 15:1353–1362
18. Kaji R (2001) Basal ganglia as a sensory gating devise for motor control. J Med Invest 48:142–146
19. Schmidt KE, Linden DEJ, Goebel R, Zanella FE, Lanfermann H, Zubcov AA (2003) Striatal activation during blepharospasm revealed by fMRI. Neurology 60:1738–1743
20. Perlmutter JS, Stambuk MK, Markham J, et al. (1997) Decreased [18F] spiperone binding in putamen in idiopathic focal dystonia. J Neurosci 17:843–850
21. Gao JH, Parson LM, Bower JM, Xiong J, Li J, Fox PT (1996) Cerebellum implicated in sensory acquisition and discrimination rather than motor control. Science 272:545–547
22. Aramideh M, Ongerboer de Visser BW, Holstege G, Majoie CBLM, Speelman JD (1996) Blepharospasm in association with a lower pontine lesion. Neurology 46:476–478
23. LeDoux MS, Brady KA (2003) Secondary cervical dystonia associated with structural lesions of the central nervous system. Mov Disord 18:60–69

Geriatr Gerontol Int 2007; 7: 124–130

Correlation between each task of the Mini-Mental State Examination and regional glucose hypometabolism in at-rest Alzheimer's disease patients

Masahiro Mishina,[1,2,3] Kenji Ishii,[2] Shin Kitamura,[3,4] Masahiko Suzuki,[2,5] Shiro Kobayashi,[1] Kiichi Ishiwata[2] and Yasuo Katayama[3]

[1]Neurological Institute, Nippon Medical School Chiba-Hokusoh Hospital, Chiba, [2]Positron Medical Center, Tokyo Metropolitan Institute of Gerontology, Tokyo, [3]The Second Department of Internal Medicine, Nippon Medical School, [4]Department of Internal Medicine, Nippon Medical School Second Hospital, Chiba, and [5]Department of Neurology, The Jikei University School of Medicine, Tokyo, Japan

We investigated the relationship between each task of the Mini-Mental State Examination (MMSE) and regional glucose hypometabolism in patients with Alzheimer's disease (AD). We studied 38 patients with probable AD using 2-^{18}F-fluoro-2-deoxy-D-glucose positron emission tomography (FDG PET). The images were corrected for differences in FDG uptake by cerebellar normalization, and were spatially normalized into a standard stereotactic anatomical space using statistical parametric mapping (SPM). There was a positive correlation between FDG uptake and the MMSE subscores for temporal orientation in the bilateral temporal and frontal cortex, and cingulate gyrus; for spatial orientation in the left parietal cortex, bilateral frontal and temporal cortex, and cingulate gyrus; for attention and calculation in the left temporal and frontal cortex; for writing in the left temporal cortex; and for copying and drawing, the correlation was positive in the bilateral parietal and occipital cortex. The total MMSE score was positively correlated with FDG uptake in the left temporal and frontal lobe. Our study demonstrated that, in AD patients, the distribution of hypometabolism in the resting state was related to clinical symptoms and that MMSE scores reflected brain dysfunction in the left hemisphere. Correlation analysis using SPM and FDG PET is useful for the objective evaluation of cognitive tests and diagnostic scoring.

Keywords: Alzheimer's disease, glucose metabolism, Mini-Mental State Examination, positron emission tomography, statistical parametric mapping.

Introduction

The cerebral glucose metabolism is thought to reflect regional neuronal activities.[1–3] Positron emission tomography (PET) with 2-^{18}F-fluoro-2-deoxy-D-glucose (FDG), and statistical image analysis applications such as statistical parametric mapping (SPM) and three-dimensional (3D) stereotactic surface projections,[4,5] have shown that the cerebral glucose metabolism in patients with Alzheimer's disease (AD) is reduced in the temporal, parietal, posterior cingulate and prefrontal regions. However, these findings did not correspond with the distribution of neuronal loss on postmortem studies.[6] In an ^{11}C-flumazenil PET study in AD, Ohyama *et al.*[7] showed that neuronal density was less impaired than neuronal function assessed by the

Accepted for publication 7 November 2006.

Correspondence: Dr Masahiro Mishina MD, Neurological Institute, Nippon Medical School Chiba Hokusoh Hospital, 1715 Kamagari, Inba-mura, Inba-gun, Chiba 270-1694, Japan.
Email: mishina@nms.ac.jp

cerebral blood flow and glucose metabolism in the associated cortex. This discrepancy may be attributable to the observation that most of the cerebral glucose metabolism reflects the synaptic activities projecting from neurons.[1,8] Based on this hypothesis, FDG PET can be used for brain-function mapping.[9-11] Recent image analysis applications, such as SPM, allow us to analyze all available metabolic information, without a priori hypotheses based on anatomic knowledge which is essential for regions of interest (ROI) analysis.[12,13] In patients with brain damage, it is possible to calculate the region at which there is a correlation between the functional disturbance and glucose hypometabolism.[14]

The Mini-Mental State Examination (MMSE) is the most commonly used method to evaluate cognitive function and to screen for dementia.[15] Some studies reported the regional glucose hypometabolism of AD correlated with total score of MMSE,[4,16] and neuropsychological subjects.[17-21] However, no data are available on the relationship between each task in the MMSE and the regional brain dysfunction of AD. Taking into consideration each MMSE parameter, we used MMSE subscores and FDG PET to investigate the relationship between the cognitive tasks of MMSE and regional glucose hypometabolism in AD patients.

Materials and methods

Subjects

We retrospectively evaluated 117 consecutive AD patients who underwent FDG PET at the Positron Medical Center of Tokyo Metropolitan Institute of Gerontology between January 2001 and December 2004. Their diagnosis was based on criteria promulgated by the National Institute of Neurological and Communicative Diseases and the Stroke/Alzheimer's Disease and Related Disorders Association (NINCDS-ADRDA).[22] Inclusion criteria were the availability of MMSE total and subscores. Based on the results of the MMSE, performed within 1 week of PET scanning, we selected 38 patients with probable AD for this study. They were 18 men and 20 women ranging in age 59–86 years (mean, 73.3 ± 6.3). Mean of the duration of AD was 4.2 ± 3.5 years (0.7–17). Values of the age and duration were used as the nuisance variable of ANCOVA.[6,23,24] Normal subjects were not included as controls in this study.

The study protocol was approved by the Ethics Committee of the Tokyo Metropolitan Institute of Gerontology; prior written informed consent was obtained from all study participants.

Positron emission tomography imaging

Positron emission tomography was performed with an SET-2400 W scanner (Shimadzu, Kyoto, Japan) at the Positron Medical Center of Tokyo Metropolitan Institute of Gerontology;[25] all subjects had fasted for more than 5 h prior to scanning. Transmission data were acquired with a rotating $^{68}Ga/^{68}Ge$ rod source for attenuation correction. The FDG uptake was acquired with static scans after the injection of 120 MBq of FDG. During the tracer-accumulation phase, the patients remained supine, quiet and motionless in a dimly lit room; their eyes and ears were open. At 45 min post-injection, a 12-min emission scan was obtained in the 3D mode. The blood glucose concentration was measured before and after the scanning to confirm its stability during the course to the PET recordings.

Data analysis

Image manipulations were carried out on an O2 workstation (Silicon Graphics, Mountain View, CA, USA) and a PowerBook G4 (Apple Computer, Cupertino, CA, USA), using the medical image-processing application package Dr View version 5.3.1 (Asahi Kasei Joho System, Tokyo, Japan) and SPM2 (Wellcome Department of Cognitive Neurology, Institute of Neurology, London, UK) implemented in MATLAB version 5.6.1 (Mathworks, Natick, MA, USA). Using a locally produced FDG template and SPM2, the FDG images were spatially normalized into a standard stereotaxic anatomical space with a cubic (2 mm × 2 mm × 2 mm) voxel size.[12] Circular ROI 10 mm in diameter were drawn on the cerebellar hemisphere on each normalized PET image. Canonical magnetic resonance imaging (MRI) attached to SPM2 was also used to obtain information for placement of the ROI on normalized PET images. The ROI value was employed for proportional scaling. The data were corrected for individual differences in FDG uptake by proportional scaling using the cerebellar ROI value.[26] Then, the data were smoothed with a 16-mm Gaussian filter to account for residual inter-subject differences. Using SPM2 segmentation and a mean image of the MRI scan attached to SPM2, we generated a masking image of the cerebrum to remove voxels outside the cortex. With the masking image in place, we computed statistical parametric maps on a voxel-by-voxel basis using whole voxels within the brain surface to avoid missing low-metabolic brain regions. ANCOVA were also used to eliminate the effect of age and duration of the disease for each subject as the nuisance variable. The T-maps for correlations between the MMSE subscores and the FDG uptake were obtained using a multiple regression model and displayed with a voxel threshold probability of 0.001 and an extent threshold of 300 contiguous voxels per cluster (uncorrected for multiple comparisons). For the total MMSE score, we calculated the T-map for correlations with the FDG uptake at a voxel

Table 1 Mean subscore for each Mini-Mental State Examination (MMSE) parameter in 38 patients with Alzheimer's disease

No.	Subject	Mean ± SD
1	TEMPORAL ORIENTATION – 1 point for each answer Q: "What is the: (year)(season)(date)(day)(month)?"	1.84 ± 1.48
2	SPATIAL ORIENTATION – 1 point for each answer Q: "Where are we: (state)(county)(town)(hospital)(floor)?"	2.58 ± 1.45
3	REGISTRATION – 1,2 or 3 points according to how many are repeated Name three objects: Give the patient 1 s to say each. Ask the patient to: repeat all three after you have said them. Repeat them until the patient learns all three.	2.87 ± 0.34
4	ATTENTION AND CALCULATION – 1 point for each correct subtraction Ask the patient to: begin from 100 and count backwards by 7. Stop after 5 answers (93, 86, 79, 72, 65).	1.74 ± 1.61
5	RECALL– 1 point for each correct answer The patient is asked to name the 3 objects cited above.	0.53 ± 0.98
6	NAMING (2 points) The patient is asked to identify and name a pencil and a watch.	1.95 ± 0.32
7	REPETITION (1 point) Ask the patient to: repeat the phrase "No ifs, ands, or buts."	0.79 ± 0.41
8	VERBAL INSTRUCTION (1 point for each task completed properly) The patient is asked to take a paper in the right hand, fold it in half, and put it on the floor.	2.79 ± 0.53
9	READING AND OBEYING (1 point) The patient is asked to read and obey the command "Close your eyes."	0.89 ± 0.31
10	WRITING (1 point) The patient is asked to write a sentence.	0.68 ± 0.47
11	COPYING AND DRAWING (1 point) The patient is asked to copy a complex diagram of two interlocking pentagons.	0.71 ± 0.46

threshold *P*-value of 0.05 (corrected for multiple comparisons).

Results

The mean score of the MMSE was 17.4 ± 4.4 (mean ± SD) for the 38 patients. As shown in Table 1, the MMSE subscores for temporal orientation, attention and calculation, and recall were low in many patients. On the other hand, many patients scored well for registration, naming, repetition, verbal instruction, and reading and obeying.

Table 2 summarizes the results of SPM for the correlation between FDG uptake and MMSE subscores. There was a positive correlation between the FDG uptake and MMSE subscores for temporal orientation in the left middle temporal and inferior temporal gyrus, right inferior temporal, superior frontal, middle frontal, straight and cingulate gyrus (Fig. 1a), for spatial orientation in the left angular, middle occipital, middle temporal, inferior temporal, superior temporal, inferior frontal, superior frontal, medial frontal, middle frontal, straight, cingulate gyrus, and insular gyri, inferior parietal lobe, pre-cuneus, and cuneus, right pre-cuneus, cuneus, cingulate, superior frontal, middle frontal and straight gyrus (Fig. 1b), for attention and calculation in the left superior temporal, middle temporal, inferior temporal, fusiform, parahippocampal, superior temporal, middle frontal, inferior frontal, cingulate, pre-central and inferior frontal gyrus, and hippocampus (Fig. 1c), for writing in the left inferior temporal, middle temporal, superior temporal gyrus (Fig. 1d), and for copying and drawing in the right inferior parietal, superior parietal lobe, superior occipital, angular and middle occipital gyrus, pre-cuneus, and cuneus, left superior parietal, inferior parietal lobe, angular and superior occipital gyrus, cuneus, and pre-cuneus (Fig. 1e). There was no correlation between the FDG uptake and the MMSE subscores for registration, recall, naming, repetition, verbal instruction, and reading and obeying.

The total MMSE score was positively correlated with the FDG uptake in the left inferior temporal, middle temporal, superior temporal, fusiform-, parahippocampal, supramarginal, angular, inferior frontal, middle frontal straight, medial frontal, cingulate, superior frontal, pre-central gyrus, hippocampus, orbital and insular gyri, right straight, medial frontal and cingulate gyrus, and orbital gyri (Fig. 1f, Table 3).

Table 2 Positive correlation between normalized ^{18}F-fluoro-2-deoxy-D-glucose (FDG) uptake and MMSE subscores in patients with Alzheimer's disease

Location	x	y	z	T statistics	Brodmann
MMSE no. 1 (temporal orientation)					
Left middle temporal, inferior temporal gyrus	−54	−36	−10	4.29	20, 21, 37, 22
Right inferior temporal gyrus	52	−30	−22	4.15	20, 21, 36, 37
Right superior frontal, middle frontal, straight gyrus	28	46	−20	3.93	11, 25
Right cingulate gyrus	8	−40	28	3.80	26, 23, 29
MMSE no. 2 (spatial orientation)					
Left angular, middle occipital, middle temporal gyrus, inferior parietal lobe	−56	−62	50	4.29	39, 40, 19
Left middle temporal, inferior temporal, superior temporal, inferior frontal gyrus, insular gyri	−68	−56	−4	4.13	21, 20, 38, 37, 22, 47, 45, 46
Left superior frontal-, medial frontal gyrus	−14	70	20	3.88	10
Bilateral pre-cuneus, cingulate gyrus, cuneus	−6	−66	30	3.88	18, 23, 17, 30, 7
Bilateral superior frontal-, middle frontal-, straight-, cingulate gyrus	−22	34	−20	3.74	11, 10
MMSE no. 4 (attention and calculation)					
Left superior temporal, middle temporal, inferior temporal gyrus	−48	24	−22	4.93	38,47, 46
Left middle temporal, inferior temporal, fusiform, parahippocampal-, superior temporal gyrus, hippocampus	−72	−24	−14	4.77	20, 37, 21
Left middle frontal, inferior frontal, cingulate gyrus	−52	38	24	3.92	45, 48, 46
Left pre-central, inferior frontal gyrus	−60	10	28	3.73	6, 44
MMSE no. 10 (writing)					
Left inferior temporal, middle temporal, superior temporal gyrus	−66	−58	−2	3.75	37, 20, 21, 22
MMSE no. 11 (copying and drawing)					
Right inferior parietal, superior parietal lobe, superior occipital, angular, middle occipital gyrus, pre-cuneus, cuneus	30	−80	46	4.01	7, 39, 19
Left superior parietal, inferior parietal lobe, angular, superior occipital gyrus, cuneus, pre-cuneus	−32	−68	62	3.72	7, 19, 18

Coordinates refer to the standard stereotactic space of the Montreal Neurological Institute (mm). The T-maps for FDG uptake correlations with covariates of MMSE were calculated with a voxel threshold *P*-value of 0.001 and an extent threshold of 300 contiguous voxels per cluster (uncorrected for multiple comparisons).

Discussion

Our study demonstrated that, even in the resting state, the distribution of hypometabolism was well correlated with brain dysfunction in AD patients. The results of SPM analysis indicated that the clusters for spatial orientation were larger in the left than the right hemisphere and that the clusters for temporal orientation were symmetrically distributed. Calculation was related with the FDG uptake in the left temporal and frontal cortex, writing with its uptake in the left temporal cortex, and drawing with uptake in the bilateral parietal and occipital cortex. The total MMSE score was primarily reflective of brain dysfunction in the left hemisphere.

The relationship between brain function and neuroimaging has been reported. Zahn *et al.*[27] who studied 11 AD patients found that the metabolism in the left anterior temporal, posterior inferior temporal, inferior parietal, and medial occipital areas (Brodmann areas 21/38, 37, 40 and 19, respectively) correlated with verbal and non-verbal semantic performance ($P < 0.001$, uncorrected). In the 49 patients studied by Lanctot *et al.*,[21] the right middle temporal region emerged as an important neural correlate of aggression ($P < 0.01$, uncorrected). Scarmeas *et al.*[28] who performed voxel-wise multiple regression analysis that controlled for age and clinical severity, found that cerebral blood flow (CBF) was negatively correlated with education, premorbid intelligence quotient (IQ), and life activity in their nine AD patients.

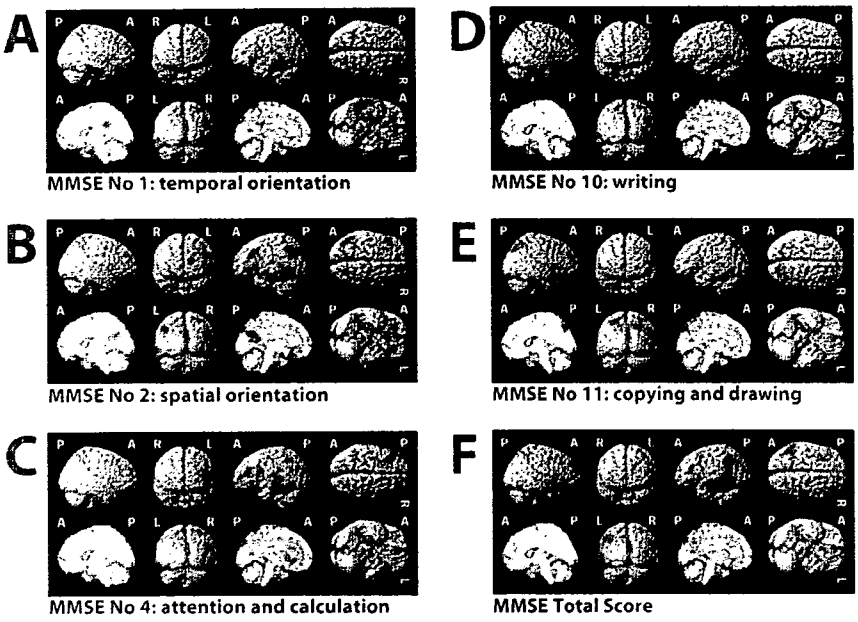

Figure 1 Statistical parametric mapping analysis of positive correlations between the regional ^{18}F-fluoro-2-deoxy-D-glucose uptake and Mini-Mental State Examination (MMSE) subscores for temporal orientation (a), for spatial orientation (b), for attention and calculation (c), for writing (d) or for copying and drawing (e), or total scores (f) in AD. T-maps are displayed with a voxel threshold probability of 0.001 and an extent threshold of 300 contiguous voxels per cluster (uncorrected for multiple comparison) for the subscores, and with a voxel threshold probability of 0.05 (corrected for multiple comparisons) for the total MMSE score.

Table 3 Correlation between normalized FDG uptake and total MMSE scores in patients with Alzheimer's disease

Location	x	y	z	T statistics	Brodmann
Positive correlation					
Left inferior temporal, middle temporal, superior temporal, fusiform, parahippocampal, supramarginal, angular gyrus, hippocampus	−56	−40	−14	7.13	20, 22, 21, 39, 38, 42, 35, 36, 37
Left inferior frontal, middle frontal gyrus	−50	34	24	4.95	45, 47, 46, 11
Bilateral straight, medial frontal, cingulate gyrus, orbital gyri	2	16	−26	4.78	11, 25
Left middle frontal, superior frontal, pre-central gyrus	−36	12	54	4.74	9, 8, 6, 46, 44
Left superior frontal, medial frontal, middle frontal gyrus	−16	64	26	4.73	10, 9
Left middle frontal gyrus	−40	56	−8	4.46	46, 47
Left insular gyri	−14	−66	−48	4.66	6
Negative correlation					
No clusters above this threshold					

Coordinates refer to the standard stereotactic space of the Montreal Neurological Institute (mm). The T-maps for FDG uptake correlations with covariates of MMSE were calculated with a voxel threshold *P*-value of 0.05 (corrected for multiple comparisons).

The results of a FDG PET study reported by Friedland *et al.*[29] suggested that drawing may be impaired in AD patients with more pronounced right than left parietal hypometabolism. In an investigation of unilateral spatial neglect in AD, single photon emission computed tomography (SPECT) revealed asymmetric perfusion of the right hemisphere.[30] Fornazzari[31] reported a painter diagnosed with early onset AD who, despite progressive cognitive impairment, retained her creativity until very late in the course of the disease although her MMSE score was 8 and she manifested a variety of cognitive difficulties such as disorientation, agnosia for common household objects, apraxia and severe memory impairment. Her SPECT scan showed hypoperfusion in the bilateral parietotemporal lobe with more impairment on the left than the right side. On the other hand,

neuropsychologically, the ability of AD patients to draw appeared to be affected by deficiencies typical of left- and right-hemisphere damage.[32] The drawings of patients with right-brain damage tend to display a piecemeal approach in which individual details, although represented well, are not placed in accurate spatial relationships with one another. Patients with left-brain damage, on the other hand, produce simplified, tremulous drawings with fewer angles.[33,34] In our study, there was a relationship between the MMSE subscore for copying and drawing and hypometabolism in the bilateral parietal and occipital lobe. The result of correlation analysis may change if simpler figures, such as those of the Alzheimer's Disease Assessment cognitive subscale are used.

Many activation studies with memory tasks and neuroimaging reported that marked activation deficits were observed in the hippocampus, frontal and temporal cortex of AD (see [35] for review). In some activation studies, the activated areas, which were not revealed in normals, were often observed as compensatory mechanisms in AD patients. The tasks were more difficult to perform for the AD patients than for the normal subjects. It is difficult to demonstrate that the difference of functional activation could be attributed to the disease, to differences in performance, or to lack of cooperation.[35] We consider that the difficulty of the tasks in MMSE was different between in normals and in AD patients, and our study did not contain normal control data. Our study demonstrated that the local hypometabolism in the resting state was correlated with poor results of MMSE in AD patients. Our approach to the brain function was similar to the studies of damaged brains rather than the activation studies. In comparison with the activation studies, our methods were simple but required more subjects. In addition, further studies will be needed for the purpose of demonstration that our result was unique to AD patients.

The clinical symptoms and the results of cognitive scoring are affected by the localization of the patient's brain damage and educational and occupational history.[28,36] In the early stage of AD, many individuals with a high education and IQ can cope with pathological brain impairments and they appear symptom-free. FDG PET makes it possible to evaluate their brain function objectively without the influence of their cognitive background. Although neuroimaging may be superior to neuropsychological testing for the early diagnosis of AD,[37] the tests are simple to administer and inexpensive. Correlation analysis using SPM and FDG PET, on the other hand, is useful for the objective evaluation of cognitive tests and diagnostic scores. Studies are underway to determine whether amyloid PET represents a potentially useful tool for the early diagnosis of AD.[38,39] Until this issue is settled, FDG PET, which reflects brain function, remains a valuable modality for the examination of patients suspected to be at risk for AD.

References

1 Magistretti PJ, Pellerin L. Cellular bases of brain energy metabolism and their relevance to functional brain imaging: evidence for a prominent role of astrocytes. *Cereb Cortex* 1996; **6**: 50–61.
2 Pellerin L, Magistretti PJ. Glutamate uptake into astrocytes stimulates aerobic glycolysis: a mechanism coupling neuronal activity to glucose utilization. *Proc Natl Acad Sci USA* 1994; **91**: 10 625–10 629.
3 Tsacopoulos M, Magistretti PJ. Metabolic coupling between glia and neurons. *J Neurosci* 1996; **16**: 877–885.
4 Herholz K, Salmon E, Perani D *et al.* Discrimination between Alzheimer dementia and controls by automated analysis of multicenter FDG PET. *Neuroimage* 2002; **17**: 302–316.
5 Minoshima S, Giordani B, Berent S, Frey KA, Foster NL, Kuhl DE. Metabolic reduction in the posterior cingulate cortex in very early Alzheimer's disease. *Ann Neurol* 1997; **42**: 85–94.
6 Mielke R, Schroder R, Fink GR, Kessler J, Herholz K, Heiss WD. Regional cerebral glucose metabolism and postmortem pathology in Alzheimer's disease. *Acta Neuropathol (Berl)* 1996; **91**: 174–179.
7 Ohyama M, Senda M, Ishiwata K *et al.* Preserved benzodiazepine receptors in Alzheimer's disease measured with C-11 flumazenil PET and I-123 iomazenil SPECT in comparison with CBF. *Ann Nucl Med* 1999; **13**: 309–315.
8 Herholz K. PET studies in dementia. *Ann Nucl Med* 2003; **17**: 79–89.
9 Harris ML, Julyan P, Kulkarni B *et al.* Mapping metabolic brain activation during human volitional swallowing: a positron emission tomography study using [^{18}F]fluorodeoxyglucose. *J Cereb Blood Flow Metab* 2005; **25**: 520–526.
10 Thiel A, Hilker R, Kessler J, Habedank B, Herholz K, Heiss WD. Activation of basal ganglia loops in idiopathic Parkinson's disease: a PET study. *J Neural Transm* 2003; **110**: 1289–1301.
11 Mishina M, Senda M, Ishii K, Ohyama M, Kitamura S, Katayama Y. Cerebellar activation during ataxic gait in olivopontocerebellar atrophy: a PET study. *Acta Neurol Scand* 1999; **100**: 369–376.
12 Friston KJ, Ashburner J, Frith CD, Poline JB, Heather JD, Frackowiak RS. Spatial registration and normalization of images. *Hum Brain Mapp* 1995; **2**: 165–168.
13 Friston KJ, Holmes AP, Worsley KJ, Poline JP, Frith CD, Frackowiak RS. Statistical parametric maps in functional imaging: a general linear approach. *Hum Brain Mapp* 1995; **2**: 189–210.
14 Mishina M, Ishii K, Mitani K *et al.* Midbrain hypometabolism as early diagnostic sign for progressive supranuclear palsy. *Acta Neurol Scand* 2004; **110**: 128–135.
15 Folstein MF, Folstein SE, McHugh PR. "Mini-mental state". A practical method for grading the cognitive state of patients for the clinician. *J Psychiatr Res* 1975; **12**: 189–198.
16 Bokde AL, Teipel SJ, Drzezga A *et al.* Association between cognitive performance and cortical glucose metabolism in patients with mild Alzheimer's disease. *Dement Geriatr Cogn Disord* 2005; **20**: 352–357.
17 Desgranges B, Baron JC, de la Sayette V *et al.* The neural substrates of memory systems impairment in Alzheimer's disease. A PET study of resting brain glucose utilization. *Brain* 1998; **121**: 611–631.

18 Desgranges B, Baron JC, Lalevee C *et al.* The neural substrates of episodic memory impairment in Alzheimer's disease as revealed by FDG-PET: relationship to degree of deterioration. *Brain* 2002; **125**: 1116–1124.
19 Newberg A, Cotter A, Udeshi M *et al.* Brain metabolism in the cerebellum and visual cortex correlates with neuropsychological testing in patients with Alzheimer's disease. *Nucl Med Comm* 2003; **24**: 785–790.
20 Kalpouzos G, Eustache F, de la Sayette V, Viader F, Chetelat G, Desgranges B. Working memory and FDG-PET dissociate early and late onset Alzheimer disease patients. *J Neurol* 2005; **252**: 548–558.
21 Lanctot KL, Herrmann N, Nadkarni NK, Leibovitch FS, Caldwell CB, Black SE. Medial temporal hypoperfusion and aggression in Alzheimer disease. *Arch Neurol* 2004; **61**: 1731–1737.
22 McKhann G, Drachman D, Folstein M, Katzman R, Price D, Stadlan EM. Clinical diagnosis of Alzheimer's disease: report of the NINCDS-ADRDA Work Group under the auspices of Department of Health and Human Services Task Force on Alzheimer's Disease. *Neurology* 1984; **34**: 939–944.
23 Sakamoto S, Ishii K, Sasaki M *et al.* Differences in cerebral metabolic impairment between early and late onset types of Alzheimer's disease. *J Neurol Sci* 2002; **200**: 27–32.
24 Hanyu H, Shimuzu T, Tanaka Y, Takasaki M, Koizumi K, Abe K. Effect of age on regional cerebral blood flow patterns in Alzheimer's disease patients. *J Neurol Sci* 2003; **209**: 25–30.
25 Fujiwara T, Watanuki S, Yamamoto S *et al.* Performance evaluation of a large axial field-of-view PET scanner: SET-2400W. *Ann Nucl Med* 1997; **11**: 307–313.
26 Soonawala D, Amin T, Ebmeier KP *et al.* Statistical parametric mapping of ^{99m}Tc-HMPAO-SPECT images for the diagnosis of Alzheimer's disease: normalizing to cerebellar tracer uptake. *Neuroimage* 2002; **17**: 1193–1202.
27 Zahn R, Juengling F, Bubrowski P *et al.* Hemispheric asymmetries of hypometabolism associated with semantic memory impairment in Alzheimer's disease: a study using positron emission tomography with fluorodeoxyglucose-F18. *Psychiatry Res* 2004; **132**: 159–172.
28 Scarmeas N, Zarahn E, Anderson KE *et al.* Association of life activities with cerebral blood flow in Alzheimer disease: implications for cognitive reserve hypothesis *Arch Neurol* 2003; **60**: 359–365.
29 Friedland RP, Koss E, Haxby JV *et al.* Alzheimer disease: clinical and biological heterogeneity. *Ann Intern Med* 1988; **109**: 298–311.
30 Ishiai S, Koyama Y, Seki K *et al.* Unilateral spatial neglect in AD: significance of line bisection performance. *Neurology* 2000; **55**: 364–370.
31 Fornazzari LR. Preserved painting creativity in an artist with Alzheimer's disease. *Eur J Neurol* 2005; **12**: 419–424.
32 Kirk A, Kertesz A. On drawing impairment in Alzheimer's disease. *Arch Neurol* 1991; **48**: 73–77.
33 Gainotti G, Tiacci C. Patterns of drawing disability in right and left hemispheric patients. *Neuropsychologia* 1970; **8**: 379–384.
34 Kirk A, Kertesz A. Hemispheric contributions to drawing. *Neuropsychologia* 1989; **27**: 881–886.
35 Prvulovic D, Van de Ven V, Sack AT, Maurer K, Linden DE. Functional activation imaging in aging and dementia. *Psychiatry Res* 2005; **140**: 97–113.
36 Scarmeas N, Zarahn E, Anderson KE *et al.* Cognitive reserve-mediated modulation of positron emission tomographic activations during memory tasks in Alzheimer disease. *Arch Neurol* 2004; **61**: 73–78.
37 Zamrini E, De Santi S, Tolar M. Imaging is superior to cognitive testing for early diagnosis of Alzheimer's disease. *Neurobiol Aging* 2004; **25**: 685.
38 Klunk WE, Engler H, Nordberg A *et al.* Imaging brain amyloid in Alzheimer's disease with Pittsburgh Compound-B. *Ann Neurol* 2004; **55**: 306–319.
39 Nordberg A. PET imaging of amyloid in Alzheimer's disease. *Lancet Neurol* 2004; **3**: 519–527.

実地病理医に必要な神経病理Ⅱ　変性・炎症・小児

【神経変性疾患】

一般内臓器の検索が神経疾患の診断に果たす役割

村山繁雄　　齊藤祐子　　池村雅子

病理と臨床・別刷

2007　vol. 25　no. 11

東京／文光堂／本郷

【神経変性疾患】

一般内臓器の検索が神経疾患の診断に果たす役割

村山繁雄[*1]　齊藤祐子[*2]
池村雅子[*3]

Ⅰ．背　　景

一般内臓器の検索が神経疾患の診断に果たす役割について考える時，脳・脊髄を含めた内臓を障害する全身疾患を対象とする場合，脳の検索は全体の一部である．ただ，臨床的に神経系の病変が全景に出ている場合，神経系に特有の病理を呈してくる点に注意が必要である．動脈硬化がその代表で，脳の血管の解剖（外弾性板を欠く）・生理学的特異性（頭蓋内血圧のオートレギュレーション）により，臨床的危険因子が，頭蓋内（高血圧＞糖尿病＞高脂血症）と頭蓋外血管（高血圧＝糖尿病＝高脂血症）で異なる．しかし例えば，血管障害性認知症の代表とされるBinswanger型白質脳症の場合，運動障害の進行と共に必須要件とされる高血圧の病歴が末期には明瞭でなくなる場合がある．その場合，全身動脈硬化が高度であること，心重量が増加していることが，診断上大きな助けになる．また，家族性アミロイドポリニューロパチーの場合，アミロイドによる心筋障害が多くの場合死因となり，心臓の検索は必須事項であるが，末梢神経近位部へのアミロイド沈着が本人の日常生活を障害し，医療機関を受診する根拠となるため，ポリニューロパチーの病名となる．

一方外科的疾患では，転移性脳腫瘍の原発巣の同定，悪性リンパ腫が脳原発かどうかの鑑別は，全身検索以外方法はない．

Parkinson病，Lewy小体型認知症，Lewy小体型自律神経不全症を含むLewy小体病は，本来中枢神経系と末梢自律神経系を侵す全身疾患である（**図1**）．現在Parkinson病を含むLewy小体病の臨床診断に，心臓交感神経節の節後機能を反映すると考えられている，MIBG（^{123}I-metaiodobenzylguanidine）心筋シンチグラフィーが本邦において汎用されている．脳の病気をなぜ心臓で診断しようとするのかについては，罹患者のみならず，非専門領域の医療関係者や，欧米諸国の医師からも，疑問が提出されている．しかし，自律神経系は全身臓器に入り込み，その調節を司っており，実質との区別は不可能である．Lewy小体病が末梢自律神経系を障害することは，既に確認されている．実際，便秘（結腸・直腸），排尿障害（膀胱），起立性低血圧（副腎交感神経節），胃・食道逆流を伴う誤嚥（胃・食道接合部），発汗低下を一因とする褥創（皮膚）等は，本来自律神経障害の結果であるが，神経内科医を含め，その背後にLewy小体関連病理が存在することを，あまり意識してこなかったことは事実である．

本稿では，最近我々が明らかにした，Lewy小体病の副腎病変について詳述する．

Ⅱ．高齢者ブレインバンクプロジェクト

老人医療センター（以下；センター）剖検病理科と，老人総合研究所（以下；研究所）神経病理部門は共同で，高齢者ブレインバンクを構築している．センター連続開頭剖検例を，ご遺族の同意のもと，研究所で国際的に最先端の手法で神経病理診断を行い，かつ凍結材料を研究資源として蓄積する試みである．諸外国のブレインバンクと異なる点は，次の3点である．①センターが在宅支援高齢者専門救急病院であるため，ご遺族および関係者がセンターの患者様であることが多く，信頼関係に基づく生前情報の収集が，後方視的に可能であること．また研究成果をご遺族に，直接還元することが容易であること．このため，資源は連結可能匿名化のもとに蓄積されている．②センター剖検例は在宅高齢者をほぼ代表しているため，疾患，コントロール以外に，その中間段階の症例を多数含み，連続

[*1]東京都老人総合研究所高齢者ブレインバンク
[*2]東京都老人医療センター剖検病理科
[*3]三井記念病院病理

0287-3745/07/¥100/頁/JCLS

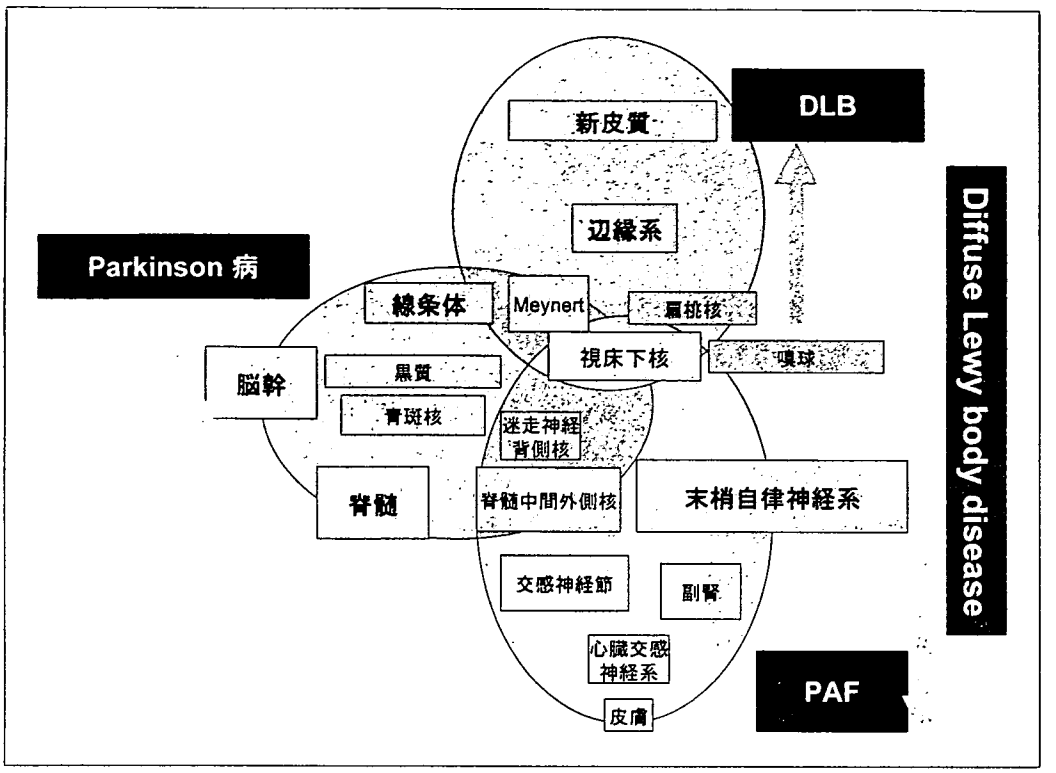

図1 Lewy小体病理
Lewy小体病は全身疾患である．DLB：dementia with Lewy bodies，PAF：Lewy-related pure autonomic failure.

的変化である老化研究が可能であること．これは，Alzheimer病を例にすれば，重度から軽度の症例，軽度認知障害（MCI）に正常コントロールまで，全てを症例として網羅していることを意味する．③欧米のブレインバンクが原則として脳のみの蓄積であるのに対し，脳以外の全身臓器を組織バンクとしてセンター病理側で蓄積しており，ブレインバンクと全身臓器との相互の連関がとれること．このブレインバンクと全身組織バンクの共同作業が本研究の前提である．

高齢者ブレインバンク症例については，原則として半脳を凍結保存，病理検索については切り出し部位35ヵ所を決め，ウェブサイト（www.mci.gr.jp/BrainBank/complete.jpg）に公開している．組織診断については，高感度鍍銀染色であるGallyas-Braak鍍銀染色，改良メセナミン銀染色に加え，Alzheimer病に代表されるアミロイドβ蛋白沈着とタウ沈着，Parkinson病に代表されるαシヌクレイン沈着，前頭側頭様型認知症に代表されるユビキチン沈着を，どの施設でも適用可能である免疫組織化学により，市販抗体で，Ventana NX20自動免疫染色装置を用い，国際診断基準に基づく半定量化を行っている[1,2]．使用抗体は，抗リン酸化タウ（AT8，Innogenetics），抗Abeta（11-28，IBL），抗αシヌクレイン（psyn #64，和光純薬），体ユビキチン抗体（Sigma）である．

上記の詳細検索と同時に，必須最小検索部位16ヵ所を，CERAD（Consortium to Establish Registry for Alzheimer Disease）とConsensus Guidelines for Dementia with Lewy bodiesを基に決定，ウェブサイトに公開（http://www.mci.gr.jp/BrainBank/essential.jpg），東京大学医学部附属病院，国立国際医療センターで，開頭剖検例全例に適用を開始している．これらは全て，普通サイズのスライドグラスを使用しての切り出しを前提とし，免疫染色だけで，老化性変化の半定量化を行っている（http://www.mci.gr.jp/BrainBank/archives/index.php）．染色条件・方法はウェブサイトに公開し，Ventana NX20を採用している大手検査会社と調整し，それぞれの施設で委託すれば同じ結果が得られる体制を全国規模で構築している．また，これら施設で共通に用いている脳肉眼所見用紙もアップロードしている．これらは全て，一般病院でも，固定条件（αシヌクレインの免疫染色には，中性緩衝ホルマリンで，2週間以内の固定が推奨される）と，切り出し部位さえ守れば，国際標準に基づく神経病理診断が可能である体勢の構築を目指したものである．Alzheimer病は高齢者の約10%，Lewy小体病は高齢者の約2%に認められ，このような頻度の高い疾患を，専門神経病理研究施設でのみで検索するには，無理があるからである．

Ⅲ．全身疾患としてのLewy小体病における副腎の位置づけ

Lewy小体病が全身疾患であることが，病理学的に強調されてこなかった最大の理由は，HE染色によりLewy小体をみつけるのは末梢自律神経系ではしばしば困難であること，交感神経節が検索の必須組織と考えられてきたが，剖検時専門的採取が必要であることの2点である．Lewy小体の主要構成成分であるリン酸化αシヌクレインに対する抗体を用いた免疫染色で，検出特異度・感度の問題は解決可能となった．残る問題として，一般病理における通常検索部位で，交感神経節の代用ができないかである．この点で，発生学的に交感神経節相同臓器である副腎に注目した．

副腎髄質は胎生7週頃に神経堤から遊走してきた交感神経系の細胞が，副腎皮質原基に進入することで形成され，軸索突起をもたない内分泌型の細胞へと分化し形成される．神経節細胞自体も髄質内にみられ，また，同じく神経堤に由来しながら，副腎皮質原基に進入せずに形成された，傍副腎神経節が副腎周囲に散在している．

Ⅳ．対象と方法

1．対　象

センター連続開頭剖検例（1999年10月～2006年3月）783例［男性455例，女性328例，死亡時平均年齢80.7±8.8歳（48～104歳）］，平均死後時間13時間10分±6時間36分を対象とした．これらの症例は，死後1時間以内に冷蔵庫に移されている結果，死後変化が少ないのが特徴である．

2．臨床・病理

副腎に関しては，10%緩衝ホルマリン固定後両側の副腎最大割面をパラフィン包埋し，3μmあるいは6μm厚の切片を作製した．脱パラフィン後，HE染色を施行した．

Parkinson症状，認知症の有無は病歴を参照した．中枢神経系の病理評価は前述した高齢者ブレインバンクプロトコールに従って行った．全例において中枢神経系Lewy小体ステージを，Lewy小体の進展範囲で，脳幹型（B），移行型（T），新皮質型（N），扁桃核亜型（A）に分類すると共に，神経原線維変化，老人斑，嗜銀顆粒のステージ分類を行った．

3．免疫組織化学

副腎については，中枢神経系検索に用いた抗体に加え，抗リン酸化αシヌクレイン（pSyn）抗血清（PSer129），抗tyrosine hydroxylase（TH）抗体（monoclonal，Calbiochem-Novabiochem Corporation，Darmstadt，Germany），抗リン酸化neurofilament抗体（SMI31，monoclonal，Sternberger Immunochemicals，Bethesda，Maryland，USA）を併用した．

Ⅴ．結　果

1．中枢神経系のLewy小体病理

783例のLewy小体の高齢者ブレインバンクステージは，ステージ0（Lewy構造なし）：577例，ステージ0.5（Lewy突起のみ）：36例，ステージⅠ（偶発的Lewy小体病＝Lewy小体はあるが，黒質の脱色素なし）：85例，ステージⅡ（発症前Lewy小体病＝Lewy小体に関連した黒質の脱色素あるが，Lewy小体に関連したParkinson症状，認知症の記載なし）：29例，ステージⅢ（認知症を伴わないParkinson病：PDN）：4例，ステージⅣ（認知症を伴うParkinson病（PDD）あるいはLewy小体型認知症（DLB）で，Lewyスコアが移行型）：27例，ステージⅤ（PDD/DLBで，Lewyスコアが新皮質型）：25例であった．ステージⅠの85例に進展分類を施すと，ⅠB（脳幹型）：41例，ⅠT（移行型）：35例，ⅠA（扁桃核亜型）：9例となり，ステージⅡの29例ではⅡB：5例，ⅡT：19例，ⅡN（新皮質型）：2例そしてⅡA：3例であった．

2．副腎におけるLewy小体病理

783例中87例（11.1%）に副腎にLewy小体病理を認め，出現部位として，①副腎髄質内神経節細胞（**図2**），②副腎皮質の間質を通る神経束，③副腎被膜脂肪組織内神経節（**図3**），④副腎被膜脂肪組織内神経束（**図4**）の4ヵ所が同定できた．なお，副腎小体はαシヌクレインに対するいずれの抗体でも陰性であった．

副腎被膜脂肪組織内神経節細胞および副腎髄質神経節細胞はいずれも，交感神経のマーカーとして知られる抗TH抗体陽性であった．副腎被膜脂肪組織内神経節では，突起内Lewy小体を多数認めたが，この点は交感神経節と共通していた．副腎髄質内神経節細胞も同様の特徴を示した．神経節細胞以外の副腎髄質細胞内にLewy小体は認めなかった．副腎被膜脂肪組織内神経束にはpSyn陽性となる点状・線状の陽性所見が散見され，少数ではあるが腫大突起としてHE染色で認識可能で，同部はpSyn陽性，辺縁がSMI31陽性で

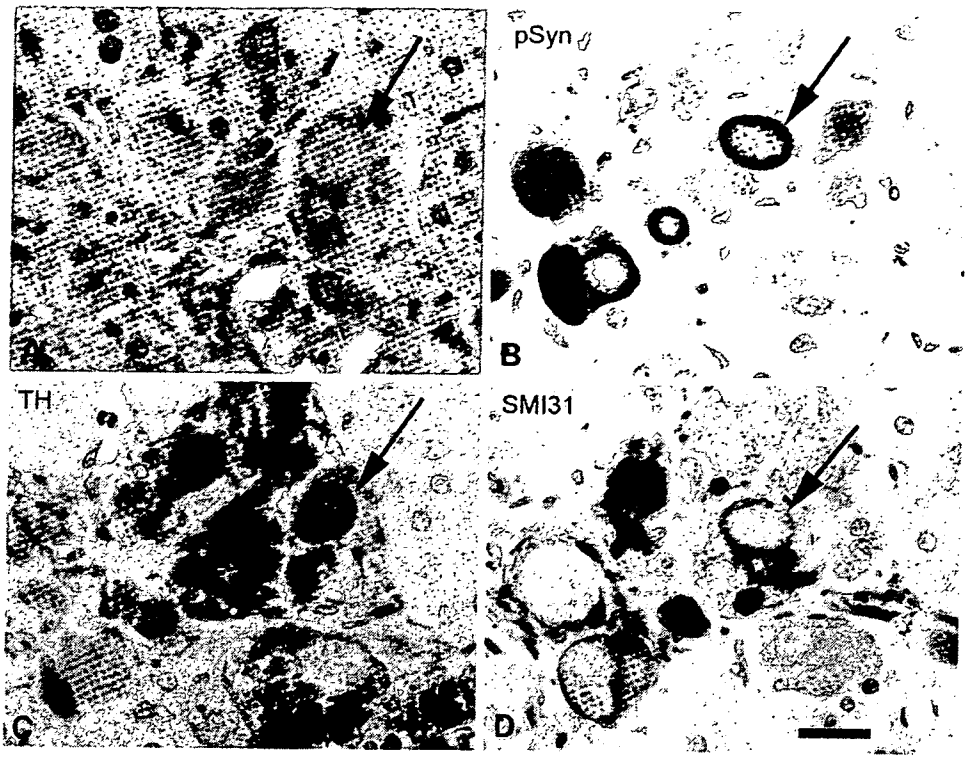

図2　副腎髄質内神経細胞のLewy小体病理　A：HE染色，B：抗リン酸化αシヌクレイン抗体(pSyn #64)免疫染色，C：抗tyrosine hydroxylase(TH)抗体免疫染色，D：抗リン酸化neurofilament抗体(SMI31)免疫染色．髄質・皮質境界部の神経節細胞内や周囲の突起内にpSyn免疫染色陽性所見を認め(B)，その一部はHE染色でも確認できる(A)．pSyn陽性構造をもつ細胞は，抗TH抗体免疫染色で陽性となるが，SMI31免疫染色では，Lewy小体形成部位で特に中心の染色性が低下し，辺縁部のみに陽性所見を認める．Lewy小体病理はSMI31免疫染色陽性細胞にのみ認められ，神経節細胞以外の髄質細胞内にはみられない(文献5より一部改変)．bar＝25μm.

あった．

副腎にLewy小体病理を認めた87例について，①②を副腎実質内，③④を副腎実質外として比較を行うと，実質内陽性は87例中60例(69.0%)，実質外陽性は87例中86例(98.8%)とほぼ全例であった．

免疫組織化学的所見を基に，HE染色を見直した場合，免疫染色陽性でHE色でも確認できるものが87例中37例，確認できないものが50例で，免疫染色の併用で感度がほぼ2.5倍に上昇していることがわかった．

3. 副腎と中枢神経系のLewy小体病理の関係

中枢神経系Lewy小体各ステージにおける，副腎Lewy小体病理の出現頻度は，認知症の有無にかかわらず，Parkinson病では100%であった．また中枢神経系にLewy小体病理を認めない1例，極少数のLewy突起を認める1例で，副腎に明らかな陽性所見をみた．

ステージI(偶発的Lewy小体病)・II(発症前Lewy小体病)において，亜型別副腎Lewy小体病理陽性率は，IB(脳幹型)：16/41例(39.0%)，IT(移行型)：8/35例(22.9%)，IA(扁桃核亜型：0/9例(0%)．ステージIIに関しては，IIB：4/5例(80%)，IIT：14/19例(73.7%)，IIN：2/2(100%)，IIA：0/3例(0%)であった．扁桃核亜型は，Alzheimer病との老年性認知症疾患に続発し，扁桃核優位にLewy小体が誘発された病型であり，Parkinson病とは発症機序が異なると考えられているが，副腎にLewy小体病理を伴わない点で，Parkinson病とは明らかに区別された．

ステージIV(PDD/DLB移行型)・V(PDD/DLB新皮質型)で，副腎にLewy小体病理を認めない5例について検討を行った．臨床的にこれらの症例はいずれも認知症が初発症状であると共にParkinson症状の記載を欠いており，DLBと分類された．また，神経病理学的には5例中4例にAlzheimer病の病理を，1例に嗜銀顆粒性認知症の病理を合併していた．

VI. 考　　察

副腎の検討により以下の点が明らかとなった．①認知症の有無にはかかわらず，Parkinson病では副腎にLewy小体病理が必発である．②他の老年性変化に続発するとされる扁桃核亜型では，副腎にLewy小体病理はみられない．③DLBのうち，副腎にLewy小体病理を認めない症例は，Alzheimer病あるいは嗜銀顆粒性認知症の病理を合併しており，Parkinson症状の記載を欠く．④中枢神経系のLewy小体関連病理が非常に軽微であるか全く認めないにもかかわらず，副腎にLewy小体病理を明らかに認める症例が存在する．⑤副腎小体はLewy小体と関係はない．Lewy小体病

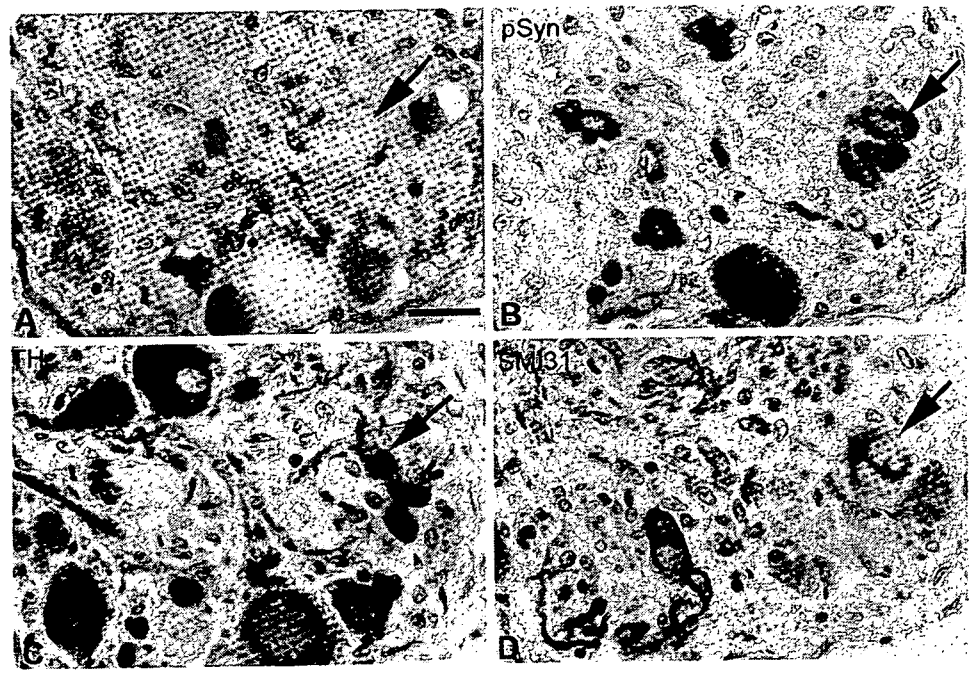

図3　副腎被膜脂肪組織内神経節のLewy小体病理　A：HE染色，B：抗リン酸化αシヌクレイン抗体（pSyn #64）免疫染色，C：抗tyrosine hydroxylase（TH）抗体免疫染色，D：抗リン酸化neurofilament抗体（SMI31）免疫染色．
副腎周囲脂肪組織内には抗TH抗体陽性となる小さな神経節が症例によって存在し，pSyn陽性所見を主に神経節細胞周囲の突起内に認めた（B）．陽性所見の一つに注目すると，HE染色においても均一な好酸性構造として認識可能であり（A），抗TH抗体においても陽性所見を示すが（C），SMI31では特に中心部において染色性の低下を認める（D）（文献5より一部改変）．bar＝25μm．

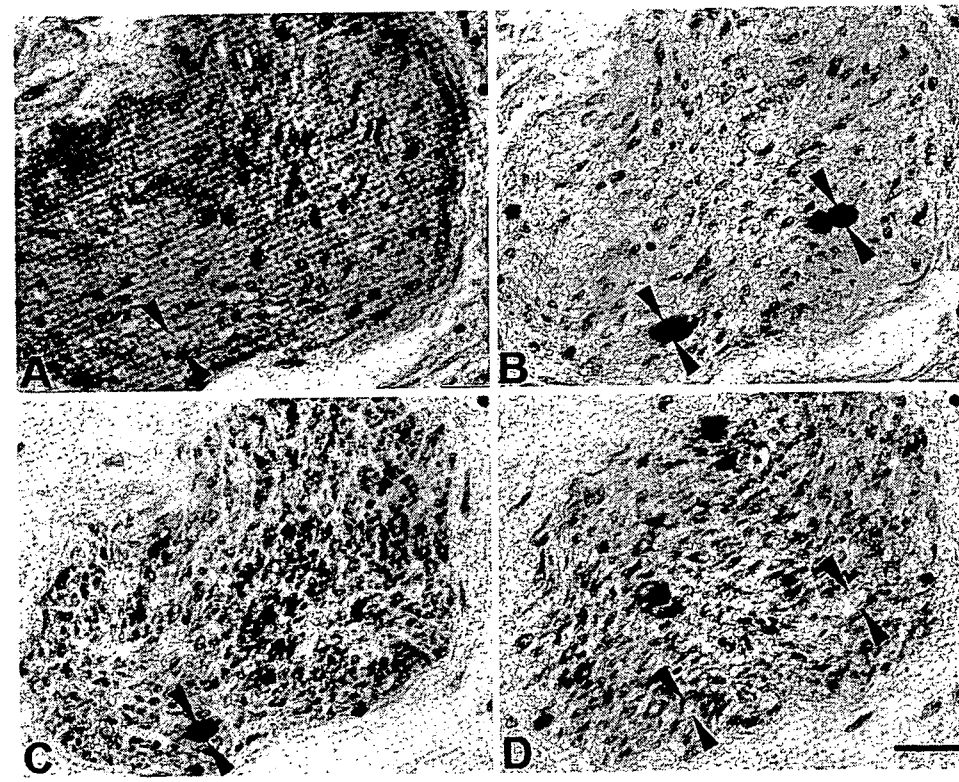

図4　副腎被膜脂肪組織内神経束のLewy小体病理　A：HE染色，B：抗リン酸化αシヌクレイン抗体（pSyn #64）免疫染色，C：抗tyrosine hydroxylase（TH）抗体免疫染色，D：抗リン酸化neurofilament抗体（SMI31）免疫染色．
副腎周囲の脂肪組織内に存在する神経束には点状，類円形の，pSyn陽性所見を認める（B）．抗TH抗体では同じ神経束が陽性となる（C）が，SMI31ではLewy小体関連病変の部位のみ染色性の低下を認める（D）．HE染色では認識できないものがほとんどだが，類円形の陽性所見の部位で，軸索腫大の形で認識可能である場合がある（A）（文献5より一部改変）．bar＝25μm．

理を発現するのは末梢自律神経系であり，副腎髄質細胞ではない．

副腎で，髄質内神経節細胞および副腎周囲交感神経節に，Lewy小体病理が認められることは既に報告されている[3]が，免疫染色を用いることにより，副腎周囲の無髄線維束や，皮質内無髄線維にも，Lewy小体病理が出現することが確認された．副腎の相同器官とされる交感神経節で，Parkinson病，DLB症例において，ほぼ100％にLewy小体関連病理が認められるとされているのに対し，副腎でのLewy小体関連病理の出現率は約30％で，LBDの末梢自律神経系の病理評価に副腎が有用であるとは言えない結果であった．し